Optimizing the Resolution of Nanohole Arrays in Metal Films for Refractive Index Sensing

Gabriela Andrea Cervantes Tellez, Aftab Ahmed, Reuven Gordon*

Department of Electrical Engineering, University of Victoria, Victoria, Canada
*corresponding author, E-mail: rgordon@uvic.ca

Abstract

We optimized the resolution of nanohole arrays in metal films for refractive index sensing by increasing the sensitivity with modifications to the hole-array parameters and by reducing the noise of the sensor system. The nanohole array parameters (including film thickness, periodicity and diameter) were first optimized by finite-difference time-domain simulations, and then fabricated and tested, showing good agreement between the two cases (theory and experiment) in terms of optimal parameters. To improve the sensitivity and to reduce the noise, the laser source wavelength was optimized (including the efficiency of the camera for detection) and the intensity was increased to reduce shot noise. A bulk resolution of 6×10^{-7} RIU was demonstrated. Due to the collinear microscope geometry and potential for multiplexing of nanohole arrays, these results are encouraging for future biosensing applications.

1. Introduction

Surface plasmon resonance (SPR) sensing is an established technology for monitoring refractive index changes due to mass loading at a surface of a metal film. Since the discovery of extraordinary optical transmission through nanohole arrays in metal films [1], it has been demonstrated that these arrays may be used for sensing applications [2-3]. Compared to Kretschmann-type SPR, sensing using the nanohole arrays is extremely promising for future technologies because it allows for: a small footprint for dense integration, a high degree of multiplexing, collinear optical detection for facile integration and combined optofluidic functionality [4-25].

The optimization of sensors includes sensitivity, resolution, reproducibility and accuracy. Sensitivity depends on the sensor output to the change in refractive index. Resolution is defined as the smallest change in refractive index that the nanohole array sensor can detect and is limited by the noise of the system [26]. Commercial SPR instruments have a resolution of 10^{-7} refractive index units (RIU) [27]. So far, the resolution of nanohole arrays has been demonstrated to be between 10^{-4}-10^{-6} RIU; however, those works used complicated optical setups [28-30].

In this work, we optimize the resolution of nanohole arrays in metal films for refractive index sensing by increasing the sensitivity with modifications to the hole-array parameters and by reducing the noise of the sensor system. We achieve a bulk resolution of 6×10^{-7} RIU. Due to the collinear microscope geometry and potential for dense multiplexing of nanohole arrays with optofluidic functionality [31-33], the results are encouraging for future biosensing applications.

2. Simulation methods and results

To have an idea of the optimal parameters for nanohole sensors, we performed comprehensive calculations of the transmission spectra of nanohole arrays using the finite-difference time-domain method (FDTD). To model the dispersive gold film a fit to the experimental data of Johnson and Christy was used [34]. The substrate was taken to have refractive index of 1.52 (for glass) and the refractive index of the background was varied to determine the sensitivity. The simulation domain used perfectly matched layer boundaries to prevent reflections and Bloch boundary conditions for the periodic structure. A plane wave source was used normally incident on the nanohole array. A frequency domain profile monitor collected the transmission through the holes in the visible and near infrared wavelength range. A mesh over-ride of 2 nm was used over the metal film, and this was confirmed to capture the surface plasmon dispersion by finite difference mode calculations. The sensitivity was determined by noting the change in the transmission characteristics for varying refractive index of the solution surrounding the holes.

Periodicity of the array, hole-diameter, and metal thickness were varied to obtain the best performance of the nanohole array sensor. FDTD simulations were carried out for hole-diameters from 140 nm to 270 nm, periodicities from 415 nm to 585 nm, and gold film thicknesses from 100 nm to 500 nm.

Fig. 1(a) shows the transmission spectrum of the optimized nanohole arrays for film thickness of 100 nm. The optimization was determined in terms of the resolution, assuming that shot noise is the dominant factor (for which the noise scales as the square root of the intensity). Considering this, the resolution, when changing the

refractive index from $n_1 = 1.330$ to $n_2 = 1.331$ will be proportional to the resolution parameter, R:

$$R = \left| \frac{I_{n1} - I_{n2}}{\sqrt{I_{n1}}} \right| \qquad (1)$$

Using Equation (1), we compare the performance between the nanohole arrays, where I_{n1} and I_{n2} are the transmission intensities for the different refractive index values. Fig. 1(b) shows that the optimal wavelength for operation is at 648 nm for this film thickness, and this occurs for a hole-diameter of 150 nm and a periodicity of 425 nm. Fig. 1(c) shows the FDTD optimization for the parameter R for nanohole arrays with diameters from 140 nm to 260 nm and periodicities from 405 nm to 565 nm on a gold thick film of 100 nm.

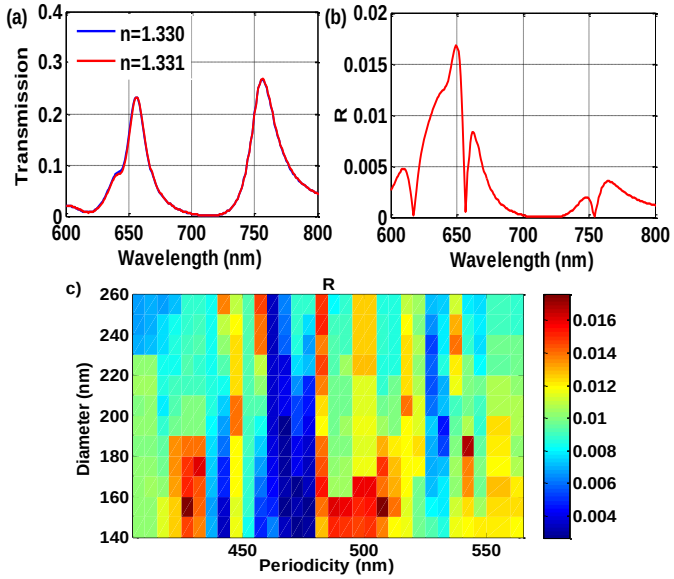

Fig. 1. Results of finite difference time domain simulations. (a) Spectrum of a circular nanohole array of a diameter of 150 nm and a periodicity of 425 nm on a gold thick film of 100 nm. (b) Optimal wavelength range for operation is at 648 nm. (c) Optimization for the parameter R for nanohole arrays with diameters from 140 nm to 260 nm and periodicities from 405 nm to 565 nm on a gold thick film of 100 nm.

It is interesting to note here that the optimal periodicity for the 100 nm film is close to the expected lowest order Bragg resonance of the plasmon dispersion for this wavelength; however, this is not the case for the thicker films. We will discuss this further in Section 6.

Fig. 2 shows equivalent results for a gold film of 300 nm thickness. The optimal parameters found were hole-diameter of 260 nm, periodicity of 570 nm. The wavelength for the best performance was 655 nm. Fig. 2(c) shows the FDTD optimization for the parameter R for nanohole arrays with diameters from 140 nm to 260 nm and periodicities from 415 nm to 585 nm on a gold thick film of 300 nm.

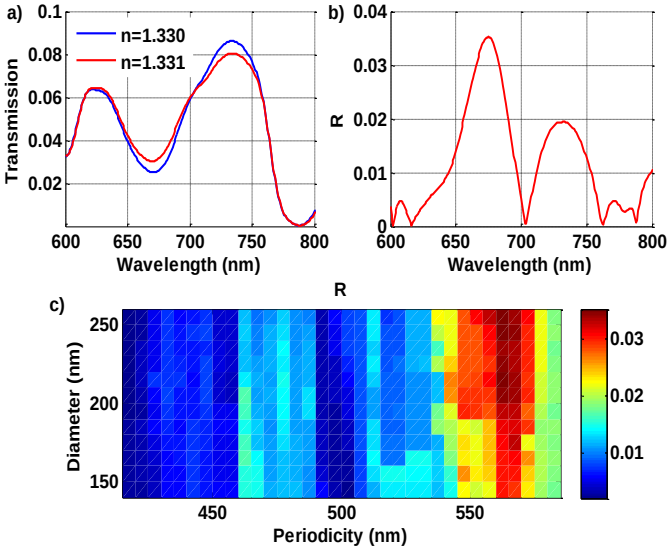

Fig. 2. Results of finite difference time domain simulations. (a) Spectrum of a circular nanohole array of a diameter of 260 nm and periodicity of 570 nm on a gold thick film of 300 nm. (b) Optimal wavelength range for operation 655 nm. (c) Optimization for the parameter R for nanohole arrays with diameters from 140 nm to 260 nm and periodicities from 415 nm to 585 nm on a gold thick film of 300 nm.

Fig. 3 shows the transmission spectrum and resolution parameter for a 500 nm gold film thickness. The optimal parameters for this thickness were hole-diameter of 260 nm and periodicity of 570 nm. The largest R value change is at the wavelength of 655 nm.

Fig. 3(c) shows the FDTD optimization for the parameter R for nanohole arrays with diameters from 140 nm to 270 nm and periodicities from 415 nm to 585 nm on a gold thick film of 500 nm.

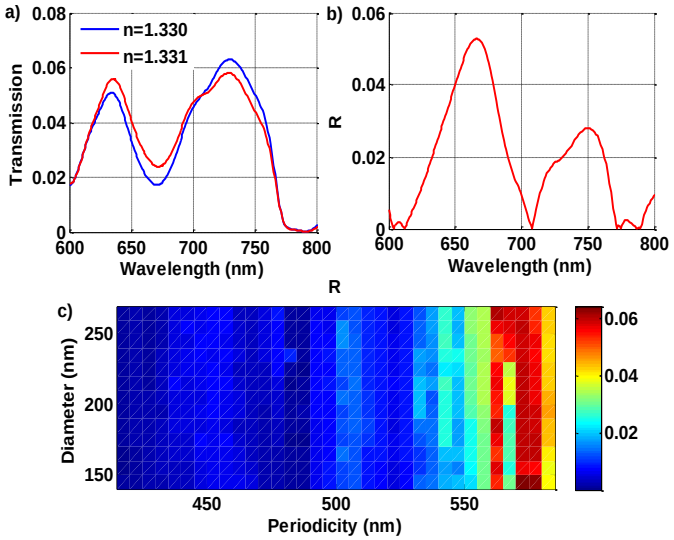

Fig. 3. Results of finite difference time domain simulations. (a) Spectrum of a circular nanohole array of a diameter of 260 nm and periodicity of 570 nm on a gold thick film of 500 nm. (b) Optimal wavelength range for operation is at 655 nm. (c) Optimization for the parameter R for nanohole arrays with diameters from 140 nm to 270 nm and periodicities from 415 nm to 585 nm on a gold thick film of 500 nm.

Comparing Figs. 1-3, it is clear that the thicker films provide better performance. In practice, however, we are limited by the ability to make high-aspect nanoholes in thick films and the duration of milling, and so we do not attempt larger thicknesses than 500 nm in this work. It is also interesting to note that the optimal wavelength of operation was consistently around 655 nm for all of the film thicknesses, and this has important ramifications for the sensor performance, as discussed further in Section 6.

3. Fabrication procedure

The nanohole arrays were fabricated by using a FB-2100 (Hitachi) focused ion beam with a gallium ion source. The ion beam was set to 40 keV for milling, and a beam current of 0.01 nA. Fig. 4 shows a scanning electron microscope image of the circular nanohole array. To match the simulations, the nanohole arrays were milled in film thicknesses of 100 nm, 300 nm and 500 nm. Due to the cost of fabrication, the simulations were used to reduce the range of fabrication parameters. For the 100 nm film thickness, the periodicity was scanned from 415 nm to 435 nm in steps of 5 nm and the diameters used were 140 nm and 160 nm. For the 300 nm and 500 nm film thicknesses, the diameters used were 260 nm and 270 nm and the periodicity was scanned from 550 nm to 580 nm in steps of 5 nm.

Good verticality of the side-walls was confirmed by energy dispersive X-ray spectroscopy studies, which showed that the gold was removed from the region of precisely (to within 5 nm) the specified radius.

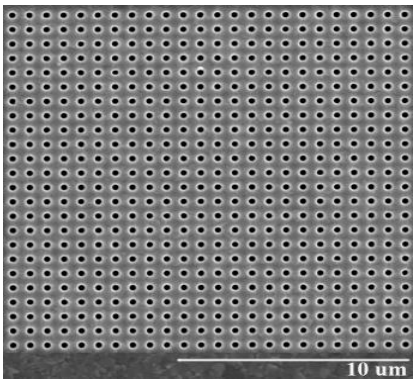

Fig. 4. Scanning electron microscope image of circular apertures with a diameter of 260 nm in a 500 nm thick gold film.

Fig. 5 shows the microfluidic chip. For measuring change in intensity due a change in the index of refraction we use a microfluidic flow channel which consists of a polydimethylsiloxane (PDMS) microchip made by rapid prototyping lithography [35]. The master mold of the channel was patterned on a silicon wafer using SU-8 50 photoresist. For the development of the microchip, a curing agent and PDMS (ratio 10:1) were used. The gold sample with PDMS flow channel was sandwiched between two acrylic layers to seal the flow channel.

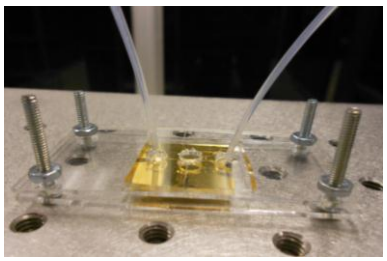

Fig. 5. Microchip of a 500 nm thick gold film sample and with PDMS microfluidic over-channel sandwiched between acrylic layers.

4. Experimental setup

Fig. 6 shows the experimental setup for measuring the fabricated gold samples. To enable scanning over a wide range of wavelengths, a supercontinuum light source (Fianium SC400) was used. With the acousto-optic tunable filter (AOTF), any desired wavelength ranging from 400 nm to 1100 nm could be obtained. This source illuminated the top surface of the sub-wavelength apertures. A spatial filter was used to improve the spatial/spectral quality of the laser beam. Two objective lenses had been set up to measure the transmission of the nanohole arrays. First, the laser beam was focused using a microscope objective of 0.1 NA, and then it was collected with a microscope objective of 0.5 NA. We experimented with various objective lens combinations, and we found that this is a good configuration. In particular, the high NA objective below the glass substrate helps to acquire a larger number of photons. By contrast, the low NA objective above the microfluidic channel ensures a low angular deviation in the incident photons, so that the

resonances (that are angle-sensitive) are more spectrally pure [36].

A CCD camera (Thorlabs DCU224C) was used to record a video of the sub-wavelength structures while flowing solutions of slightly different refractive index over the sample. Any change in the refractive index of the solution appears as a change in intensity. A syringe pump (Harvard apparatus 11 series) was used for a stable liquid flow rate of 7 µL/min.

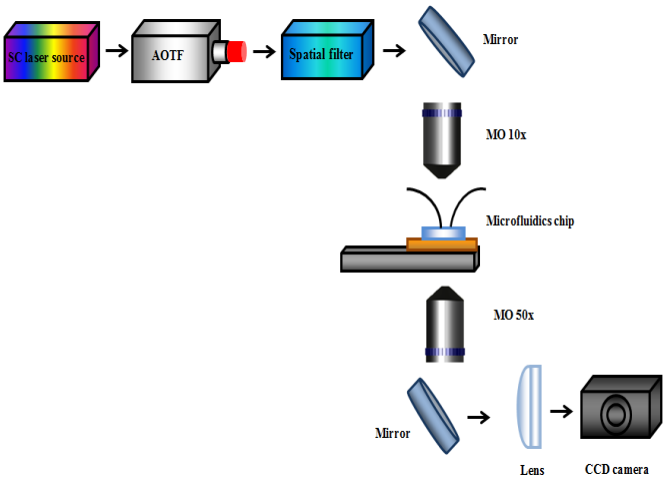

Fig. 6. Schematic of optical setup used for measuring the change in intensity of the fabricated gold samples with a super continuum laser source tunable over the visible near infrared region.

5. Results

In the experiments, the 100 nm thick gold film showed the largest sensitivity for a hole-diameter of 150 nm and periodicity of 425 nm, with a resolution of 2×10^{-6} RIU. The 300 nm thick film showed largest sensitivity for a hole-diameter of 260 nm and periodicity of 570 nm with a resolution of 8×10^{-7} RIU. The 500 nm thick film showed the largest sensitivity for a hole-diameter of 260 nm and periodicity of 570 nm, with a resolution of 6×10^{-7} RIU. These parameter values are all in close-agreement with the simulation results. It is clear also that the thicker film gives better resolution, as expected from the simulations.

Fig. 7 shows the best result obtained among all the arrays, varying the refractive index to determine the sensitivity. The curve in Fig. 7(a) has a staircase appearance because it was acquired by scanning the AOTF in 5 nm steps for 5 second duration at each step. For convenience, the figure is plotted versus wavelength instead of time.

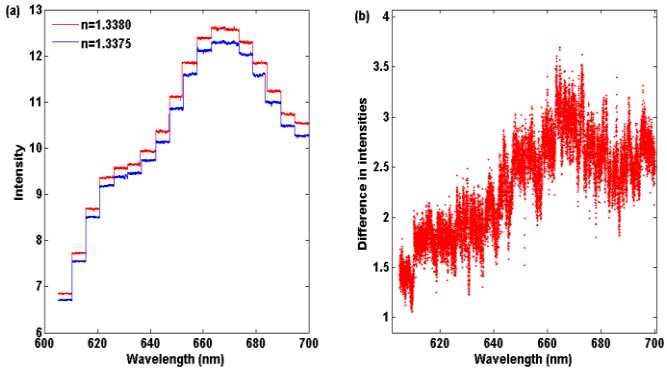

Fig. 7. (a) Representation in time of the spectrum of a nanohole array while flowing two different refractive index solutions. (b) Difference in intensities of two refractive index solutions.

Fig. 8 shows the difference in intensities of two refractive indexes values for nanohole arrays with hole-diameters of 260 nm and 270 nm and for periodicities of 550 nm and 580 nm using a 500 nm gold thick film.

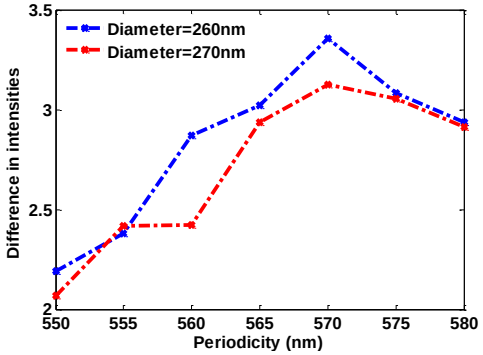

Fig. 8. Difference in intensities of two refractive indexes values for nanohole arrays with hole-diameters of 260 nm to 270 nm and for periodicities of 550 nm to 580 nm on a 500 nm gold thick film.

After choosing the optimal wavelength of operation for the nanohole array sensor measurements, by the procedure in Fig. 7, bulk sensitivity measurements were carried out with a higher intensity of 3.6 mW and using a low-pass finite impulse response numerical filter. Fig. 9 shows the intensity change of the circular nanohole arrays subjected to refractive index change of 0.0005 operating at 655 nm. The numerical filtering reduced the time resolution to 0.5 frames per second. The highest resolution that was obtained was 6×10^{-7} RIU.

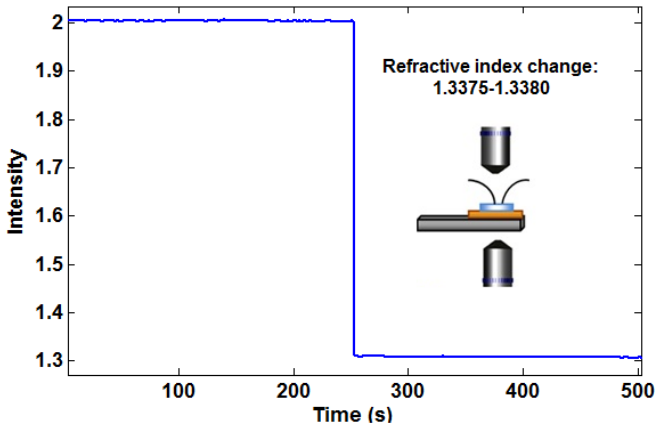

Fig. 9. Experimental results for measuring the change in intensity at 655 nm wavelength for a 500 nm thick gold film. An array of circular holes with diameter of 260 nm and periodicity of 570 nm were used.

6. Discussion

First we note that good agreement is seen between the simulation and the experiments. The achieved resolution of 6×10^{-7} RIU is a promising step towards competing with existing commercial SPR devices (10^{-7} resolution), while allowing for the integration, multiplexing and optofluidic advantages of nanohole SPR. It is interesting to note that the optimum resolution found from the simulations was around 655 nm. This is believed to result from the gold dispersion for two reasons. First, gold has a low loss at 655 nm because this wavelength is past the interband absorption peak of gold (around 510 nm). Second, the magnitude of the relative permittivity at 655 nm is not too large (it is closer to the plasma frequency than further in the IR, for example), which allows for significant electromagnetic field penetration into the metal and pronounced plasmonic effects. It is fortuitous that the optimal operation considering the material properties of gold coincides fairly well with the optimal sensitivity of the CCD camera used in this experiment (~600 nm), because this allows for higher photon collection efficiency, and therefore reduced shot-noise signal-to-noise ratio.

It is common to use the SP Bragg relation to determine the optimal periodicity for nanohole array sensing:

$$\lambda_{SP}(i,j) = p\left(i^2+j^2\right)^{-\frac{1}{2}}\left(\frac{\varepsilon_d\varepsilon_m}{\varepsilon_d+\varepsilon_m}\right)^{1/2} \qquad (2)$$

where ε_m and ε_d are the permittivities of metal and dielectric material, p is the periodicity, i and j are integers that represent Bragg resonance orders. This gives reasonable results for predicting the resonance wavelength for thinner films for the lowest order resonance. For example, the $i=0$, $j=1$ resonance of the 100 nm film with 425 nm periodicity on the water side is predicted to be 625 nm, and was observed to be 648 nm in the simulations. We see here, however, that larger periodicities are required for thicker films, and these do not seem to match the lowest order resonance. Indeed, they are closer to the $i=1$, $j=1$ resonance. The reason for this effect is still under investigation; however, this shows that future investigations should not simply chose the lowest order resonance wavelength as has been done in the past [37].

7. Conclusions

We optimized the resolution of circular nanohole arrays in metal films for refractive index sensing by increasing the sensitivity with modifications to the hole-array parameters (film thickness, periodicity and diameter), by determining the optimal wavelength of operation, and by reducing the noise of the sensor system (through increased collection efficiency, increased intensity and numerical filtering). We achieve a bulk resolution of 6×10^{-7} RIU. Due to the collinear microscope geometry, the potential for multiplexing of nanohole arrays and improved optofluidic functionality [32], these results are encouraging for future detection of chemical and biological species.

Acknowledgements

The authors are grateful for the support of the NSERC Strategic Network for Bioplasmonic Systems (Biopsys).

References

[1] T.W. Ebbesen, H.J. Lezec, H.F. Ghaemi, T. Thio, P.A. Wolff, Extraordinary optical transmission through sub wavelength hole arrays, *Nature* 391:667-669, 1998.

[2] W.L. Barnes, A. Dereux, T.W. Ebbesen, Surface plasmon subwavelength optics, *Nature* 424:824-830, 2003.

[3] A.G. Brolo, R. Gordon, B. Leathem, K.L. Kavanagh, Surface plasmon sensor based on the enhanced light transmission through arrays of nanoholes in gold films, *Langmuir* 20:4813-4815, 2004.

[4] R. Gordon, D. Sinton, K.L. Kavanagh, A.G. Brolo, A new generation of sensors based on extraordinary optical transmission, *Acc. Chem. Res.* 41:1049-1057, 2008.

[5] A. Lesuffleur, H. Im, N.C. Lindquist, S.H. Oh, Periodic nanohole arrays with shape-enhanced plasmon resonance as real–time biosensors, *Appl. Phys. Lett.* 90:243110, 2007.

[6] W.L. Barnes, W.A. Murray, J. Dintinger, E. Devaux, T.W. Ebbesen, Surface plasmon polaritons and their role in the enhanced transmission of light through periodic arrays of subwavelength holes in metal film, *Phys. Rev.* 92:107401, 2004.

[7] A. Lesuffleur, H. Im, N.C. Lindquist, K.S. Lim, S.H. Oh, Laser-illuminated nanohole arrays for multiplex plasmonic microarray sensing, *Opt. Express* 16:219-224, 2008.

[8] L. Pang, G.M. Hwang, B. Slutsky, Y. Fainman, Spectral sensitivity of two-dimensional nanohole array surface plasmon polariton resonance sensor, *Appl. Phys. Lett.* 91:123112, 2007.

[9] R. Gordon, A. G. Brolo, D. Sinton, K. L. Kavanagh, Resonant optical transmission through hole-arrays in metal films: Physics and applications, *Laser and Photonics Reviews* 4:311-335, 2010.

[10] J. Homola, S. Yee, G. Gauglitz, Surface plasmon resonance sensors: Review, *Sensor Actuat. B-Chem.* 54:3-15, 1999.

[11] A. De Leebeeck, L.K.S. Kumar, V. de Lange, D. Sinton, R. Gordon, A.G. Brolo, On-chip surface-based detection with nanohole arrays, *Anal. Chem.* 79:4094-4100, 2007.

[12] H. Gao, J. Henzie, T.W. Odom, Direct evidence of surface plasmon-mediated enhanced light transmission through metallic nanohole arrays, *Nano Lett.* 6:2104-2108, 2006

[13] N.C. Lindquist, A. Lesuffleur, H. Im, S.H. Oh, Sub-micron resolution surface plasmon resonance imaging enable by nano-hole arrays with surrounding Bragg mirrors for enhanced sensitivity and isolation, *Lab Chip* 9:382-387, 2009.

[14] Y. Liu, S. Blair, Fluorescence enhancement from an array of subwavelength metal apertures, *Opt. Express* 28:507-509, 2003.

[15] J. Dintinger, S. Klein, T.W. Ebbesen, Molecule-surface plasmon interaction in hole arrays: Enhanced absorption, refractive index changes, and all-optical switching, *Adv. Mater* 18:1267-1270, 2006.

[16] J.C. Sharpe, J.S. Mitchell, L. Lin, N. Sedoglavich, R.J. Blaikie, Gold nanohole array substrates as immunobiosensors, *Anal. Chem.* 80:2244-2249, 2008.

[17] T. Allsop, R. Neal, E.M. Davies, C. Mou, P. Bond, S. Rehman, K. Kalli, D.J. Webb, P. Calverhouse, I. Bennion, Low refractive index gas sensing a surface plasmon resonance fibre device, *Meas. Sci. Technol.* 21:094029, 2010.

[18] J. Ji, J.G. O'Connell, D.J. Carter, D.N. Larson, High-throughput nanohole array based system to monitor binding events in real time, *Anal. Chem.* 80:491-498, 2008.

[19] X. Shou, A. Agrawal, A. Nahata, Role of metal film thickness on the enhanced transmission properties of a periodic array aperture, *Opt. Express* 13:9834-9840, 2005.

[20] P.R.H. Stark, A.E. Halleck, D.N. Larson, Short order nanohole arrays in metals for highly sensitive probing of local indices of refraction as the basis for a highly multiplexed biosensor technology, *Methods* 37:37-47, 2005.

[21] K.L. Lee, S.H. Wu, P.K. Wei, Intensity sensitivity of gold nanostructures and its application for high-throughput biosensing, *Opt. Express* 17:23104-23113, 2009.

[22] C.J. Alleyne, A.G. Kirk, R.C. McPhedran, N.A.P. Nicorovici, D. Maystre, Enhanced SPR sensitivity using periodic metallic structures, *Opt. Express* 15:8163-8169, 2007.

[23] J. Homola, Present and future of surface plasmon resonance biosensors, *Anal. Bional. Chem.* 377:528-539, 2003.

[24] T. Akimoto, S. Sasaki, K. Ikebukuro, I. Karube, Refractive-index and thickness sensitivity in surface plasmon resonance spectroscopy, *Appl. Optics* 38:4058-4064, 1999.

[25] A. Dhawan, M.D. Gerhold, J.F. Muth, Plasmonic structures based on subwavelength apertures for chemical and biological sensing applications, *IEEE Sens. J.* 8:942-950, 2008.

[26] J. Homola, Surface plasmon resonace based sensors for detection of chemical and biological species, *Chem. Rev.* 108:462-493, 2008.

[27] Biacore www.biacore.com

[28] A.K. Tetz, L. Pang, Y. Fainman, High-resolution surface plasmon resonance sensor based on linewidth-optimized nanohole array transmittance, *Opt. Express* 31:1528-1530, 2006.

[29] A-P. Blanchard-Dionne, L. Guyot, S. Patskovsky, R. Gordon, M. Meunier, Intensity based surface plasmon resonance sensor using a nanohole rectangular array, *Opt. Express* 19:15041-15046, 2011.

[30] C. Escobedo, S. Vincent, A.I.K. Choudhury, J. Campbell, A.G. Brolo, D. Sinton, R. Gordon, Integrated nanohole array surface plasmon resonance sensing device using a dual-wavelength source, *J. Micromech. Michroeng.* 21:115001, 2011.

[31] C. Escobedo, A.G. Brolo, R. Gordon, D. Sinton, Optofluidic concentration: Plasmonic nanostructure as concentrator and sensor, *Nano Lett.* ASAP 2012.

[32] F. Eftekhari, C. Escobedo, J. Ferreira, X. Duan, E.M. Girotto, A.G. Brolo, R. Gordon, D. Sinton, Nanoholes as nanochannels: Flow-through plasmonic sensing, *Anal. Chem.* 81:4308-4311, 2009.

[33] C. Escobedo, A.G. Brolo, R. Gordon, D. Sinton, Flow-through vs flow over: Analysis of transport and binding in nanohole array plasmonic biosensors, *Anal. Chem.* 82:10015-10020, 2010.

[34] P.B. Johnson, R.W. Christy, Optical constants of the noble metals, *Phys. Rev. B* 6:4370, 1972.

[35] D.C. Duffy, J.C. McDonald, O.J.A. Schueller, G.M. Whitesides, Rapid prototyping of microfluidic systems in poly(dimethylsiloxane), *Anal. Chem.* 70:4974-4984, 1998.

[36] H.F. Ghaemi, T. Thio, D.E. Grupp, T.W. Ebbesen, H.J. Lezec, Surface plasmons enhance optical transmission through subwavelength holes, *Phys. Rev. B* 58:6779-6782, 1998.

[37] A. Krishnan, T. Thio, T. J. Kim, H. J. Lezec, T. W. Ebbesen, P. A. Wolff, J. Pendry, L. Martin-Moreno, F. J. Garcia-Vidal, Evanescently coupled resonance in surface plasmon enhanced transmission, *Opt. Commun.* 200:1-7, 2001.